



Showcasing research from Associate Professor Ariyoshi's laboratory, Toyohashi University of Technology, Aichi, Japan, and Associate Professor Hiroshiba's laboratory, Osaka Institute of Technology, Osaka, Japan.

Temperature dependent poly(L-lactide) crystallization investigated by Fourier transform terahertz spectroscopy

Temperature dependent poly(L-lactide) (PLLA) crystallization was investigated by Fourier transform THz spectroscopy. Characteristic PLLA absorption peaks were identified at 1.8, 4.0, 4.7, and 7.1 THz for 80 °C sample. The higher two peaks (4.7 and 7.1 THz) were attributed to the intermolecular vibration of the PLLA chain. The 4.0 THz peak was attributed to a novel intramolecular vibration and intrinsically in α -form. Broadband THz spectroscopy is a powerful tool for biodegradable polymers.

As featured in:



See Seiichiro Ariyoshi,
Nobuya Hiroshiba *et al.*,
Mater. Adv., 2021, 2, 4630.

Cite this: *Mater. Adv.*, 2021,
2, 4630

Temperature dependent poly(L-lactide) crystallization investigated by Fourier transform terahertz spectroscopy†

Seiichiro Ariyoshi,^{id}*^a Satoshi Ohnishi,^a Hikaru Mikami,^a Hideto Tsuji,^{id}^a
Yuki Arakawa,^{id}^a Saburo Tanaka^a and Nobuya Hiroshiba*^b

Poly(L-lactide) (PLLA) was investigated by Fourier transform terahertz (THz) spectroscopy over the frequency range of 1.0–8.5 THz. THz absorption spectra were acquired for PLLA samples isothermally crystallized at the temperature of 80–140 °C after melt-quenching. Characteristic PLLA absorption peaks were identified at 1.8, 4.0, 4.7, and 7.1 THz for the 80 °C sample; higher crystallization temperature resulted in a blue shift of the absorption peak frequency. The higher two peaks (4.7 and 7.1 THz), which are present not only in α -form but also in δ -form, were attributed to the intermolecular vibration of the PLLA chain, depending on the lattice spacing and crystallinity. In contrast, the 4.0 THz peak was intrinsically in α -form, thus enabling its use as an indicator in the optimization of PLLA polymorphism. Broadband THz spectroscopy is a nondestructive and noninvasive evaluation technique for biodegradable polymers.

Received 5th March 2021,
Accepted 30th May 2021

DOI: 10.1039/d1ma00195g

rsc.li/materials-advances

Introduction

Recent advances in the mass-production of polylactide (PLA) from a biomass feedstock have opened the possibility for its role as a renewable resource, specifically as an alternative to petroleum derived polymers.^{1–4} PLAs have fascinating characteristics such as piezoelectric properties and biodegradability for applications in flexible electronics.⁵ The piezoelectric constant d of PLA is approximately 7 to 12 pC N⁻¹, which is low compared to that of lead zirconium titanate (PZT). However, PLA exhibits a very low relative dielectric constant of ϵ_r (*ca.* 2.5) compared to that of PZT and polyvinylidene fluoride (PVDF).^{6,7} Therefore, the piezoelectric output constant g ($g = d/\epsilon_r$) is large when compared with that of PZT and PVDF; this reasonable sensitivity makes it a promising piezoelectric polymer material. Since the piezoelectric properties of PLA are governed by its higher-order structure, it is important to clarify the higher-order structure for the development of materials with new functions.

Recently, terahertz (THz) spectroscopy has been recognized as an attractive technique for identifying and characterizing the electrical properties and higher-order structure in polymer science. In particular, bulk properties such as intermolecular

vibration and electromagnetic interactions of photons and phonons have been investigated using boson peak analysis in the THz range that are caused by low energy excitation.⁸ In addition, THz band peak analysis is a powerful method for studying collective excited vibrations along the long polymer chain structure and entanglement.^{9–12} For instance, H. Li *et al.* reported the crystal transition of PLA. Their results indicated that the α to α' form (δ form) transformation is strongly related to a lattice vibration peak located around 2.0 THz, and the peak frequency was related to the lattice spacing derived from the X-ray diffraction (XRD) spectra.¹³ Most of their measurements used THz time-domain spectroscopy (THz-TDS) to coherently detect the THz electric field. However, this technique has a high dynamic range at low frequencies below *ca.* 3 THz,¹⁴ and the systematic analysis in the region beyond 3 THz is still limited. Fourier transform THz spectroscopy (FT-TS) is an excellent alternative for acquiring data beyond the upper frequency limit. To develop guidelines for the functional development and optimization of the piezoelectric properties of PLA materials, broadband THz analysis will also be crucial, as it reveals the relationship between higher-order structures and functional properties.

In this paper, we first explain the fabrication of poly(L-lactide) (PLLA) samples with various thermal annealing conditions for isothermal crystallization. Next, we introduce the use of broadband THz spectroscopy, which unveils the correlation between PLLA crystalline phase constitution and spectral changes. Finally, we discuss the origin of characteristic THz peaks and the usefulness of broadband THz spectroscopy.

^a Toyohashi University of Technology, 1-1 Hibarigaoka, Tempaku-cho, Toyohashi, Aichi 441-8580, Japan. E-mail: ariyoshi@tut.jp

^b Osaka Institute of Technology, 5-16-1 Omiya, Asahi-ku, Osaka, 535-8585, Japan. E-mail: nobuya.hiroshiba@oit.ac.jp

† Electronic supplementary information (ESI) available. See DOI: 10.1039/d1ma00195g



Experimental

Sample preparation

PLA is known to form the PLLA, poly(D-lactide), and their blend (or stereocomplex formation). In this experiment, PLLA samples were fabricated from pellets kindly supplied by commercial companies (UNITIKA Ltd, Japan). The pellets (product ID: 4031DK, number average molecular weight = 1.10×10^5 , and polydispersity index = 1.55, and L-lactic acid unit content = 95.2%) were first heated above the melting temperature (*ca.* 170 °C) and then pressed into a discoid shape with 0.1 mm thickness and *ca.* 20 mm diameter. After the pellets were completely melted for 90 min (200 °C), the samples were then abruptly immersed in liquid nitrogen (−196 °C) to initialize their thermal history and ensure amorphous structure. The samples were then transferred onto a hot stage pre-set at the required crystallization temperatures ($T_c = 80\text{--}140$ °C) with a 10 °C step. The temperature was maintained for 240 min to complete the isothermal crystallization process, and the samples were again immersed in liquid nitrogen to stop further crystallization.

X-Ray diffraction spectroscopy

XRD profiles were obtained using the conventional $2\theta\text{--}\theta$ scan method with an X-ray source (Cu-K $\alpha = 0.154$ nm) using a RINT-2500 diffractometer (Rigaku Corporation, Japan) in a range of 14–22° with a 0.02° step, scan speed of 4° min^{−1}, and a 40 kV, 200 mA source power.

Terahertz spectroscopy

Broadband (1.0–8.5 THz) THz spectra of the samples were measured using an FT-TS with a frequency resolution of 0.015 THz (0.5 cm^{−1}). The measurements were conducted at room temperature using a FARIS-S spectrometer (JASCO Corporation, Japan) equipped with a deuterated triglycine sulfate detector and a Martin-Puplett interferometer system including two pieces of half-mirrors, which enables a signal that is twice as strong as that obtained using conventional systems with only one half-mirror, see ESI† for further details. The samples were placed horizontally and perpendicular to the THz-wave propagation during the measurements, and the sample and interferometer spaces were evacuated to a pressure of less than 100 Pa to minimize absorption of the THz waves by oxygen gas or water vapor in the atmosphere.

Results and discussion

Absorption spectra

To investigate the relationship between the crystalline process and THz spectral features, spectral measurements were conducted on PLLA samples with different T_c from 80 °C to 140 °C. As a reference, the 80 °C sample was identified with peaks A (1.8 THz), B (4.0 THz), C (4.7 THz), and D (7.1 THz) in the relatively broad frequency range of 1.0–8.5 THz (Fig. 1(a)). A weak and broad peak appeared around 3.2 THz was not analyzed due to the mixture of multiple components. Although peaks B and C were close together, the higher T_c samples seemed to be blue-shifted, as shown in Fig. 1(b). The denser chain packing causes the higher

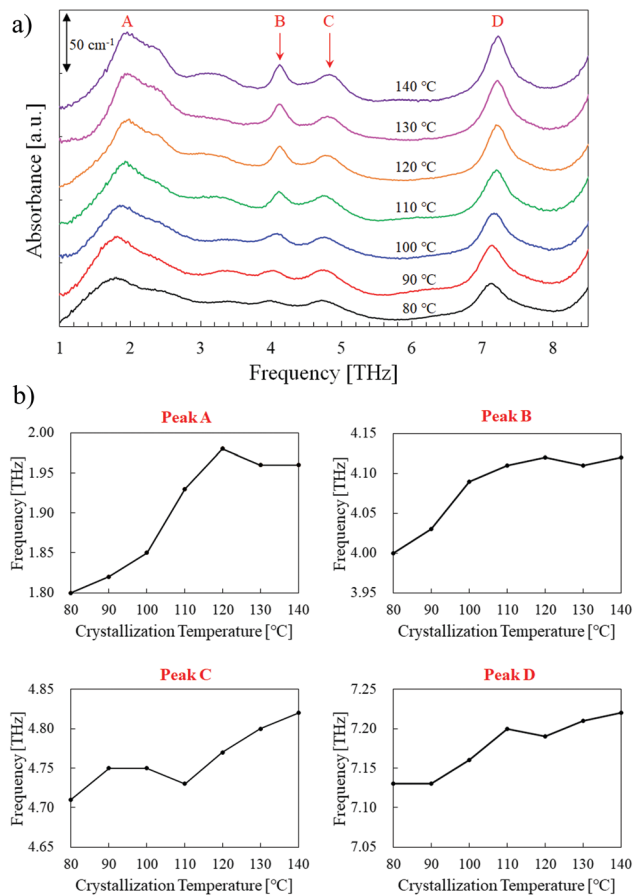


Fig. 1 (a) THz absorption spectra of PLLA for different crystallization temperature. (b) Frequency shifts of the four peaks labeled in (a).

intermolecular vibration frequency. The main origin of the blue-shift from 80 °C to 140 °C is thought to be attributed to the transition of the PLLA crystalline structure (lattice spacing) from δ -form (0.540 nm) to α -form (0.532 nm).^{15,16} A similar absorption peak around 1.8 THz only was also identified by previous researchers using THz-TDS.¹³ Our FT-TS measurements expanded the observable range and found new three peaks until 8.5 THz. The frequency shifts of peaks A and B were saturated at higher T_c , while those of peaks C and D gradually increased and did not appear to be saturated even at 140 °C. Especially, peak B seemed to be saturated at lower T_c than the other three peaks. However, no obvious difference was confirmed in peak shift behavior; therefore, further studies were required.

Spectral analysis

To quantitatively analyze the spectral change, the peak height and width (full width at half-maximum, FWHM) calculations were conducted on peaks B, C, and D. As peak A was complex by the mixture of multiple components, it was not analyzed. However, the three higher-frequency peaks had relatively simple profiles throughout the isothermal crystallization process. As an example, the peak analysis of the 80 °C sample is shown in Fig. 2. The close peaks B and C were separated by using two Gaussian fitting functions. Before this calculation, a linear baseline was



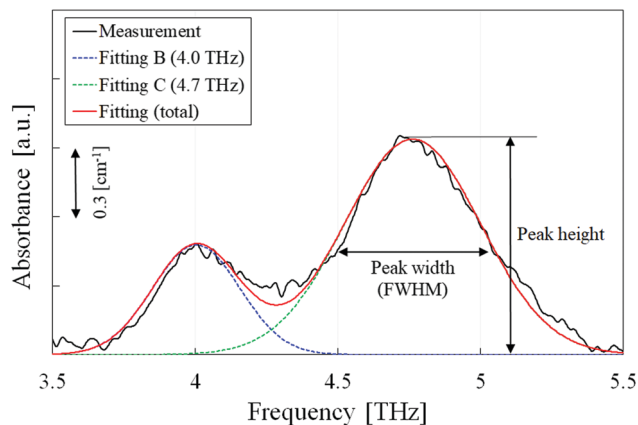


Fig. 2 Peak separation using Gaussian approximation; peaks B and C are separated to obtain the height and width for each spectrum.

adopted from 3.8 THz (the left edge of the peak B) and 5.5 THz (the valley between peaks C and D). For the single peak D, another linear baseline was employed from 6 THz (the valley between peaks C and D) and 8 THz (the right edge of peak D).

Fig. 3 shows the relative peak height and width, normalized at 80 °C, as a function of T_c . This provided a clearer and detailed description of the spectral changes in the three peaks (B, C and D). Peak C (4.7 THz) had a similar tendency as that of peak D (7.1 THz), and their relative heights and widths gradually increased and decreased with increasing T_c respectively, indicating that higher T_c samples have higher crystallinity. On the other hand, the relative height of peak B (4.0 THz) increased remarkably as the peak width slightly decreased. This tendency is consistent with XRD profiles, indicating that the sharp phase transition from δ -form to α -form was occurred around 110 °C (Fig. 4). Therefore, the relative peak intensity in THz range is an effective parameter to quantitatively evaluate the ratio of δ -form to α -form in PLLA samples. Peak B is an indicator for the optimization of polymorphism in PLLA, which would eventually influence the piezoelectric and/or biodegradable properties.

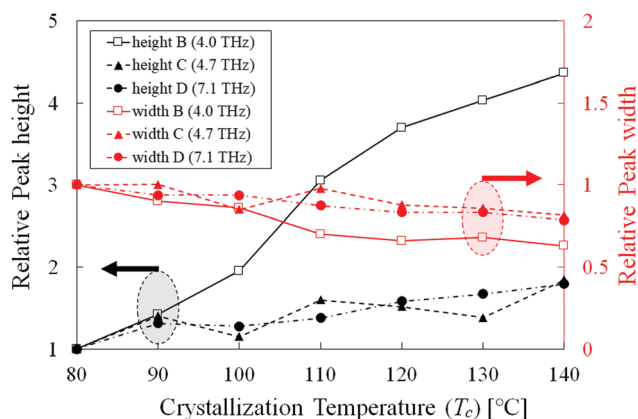


Fig. 3 Relative height and width of peaks B, C, and D plotted against the crystallization temperature, normalized at 80 °C. Absolute height (width) of peak B, C, and D at 80 °C are 4.78 cm^{-1} (0.36 THz), 9.38 cm^{-1} (0.56 THz), and 25.13 cm^{-1} (0.46 THz), respectively.

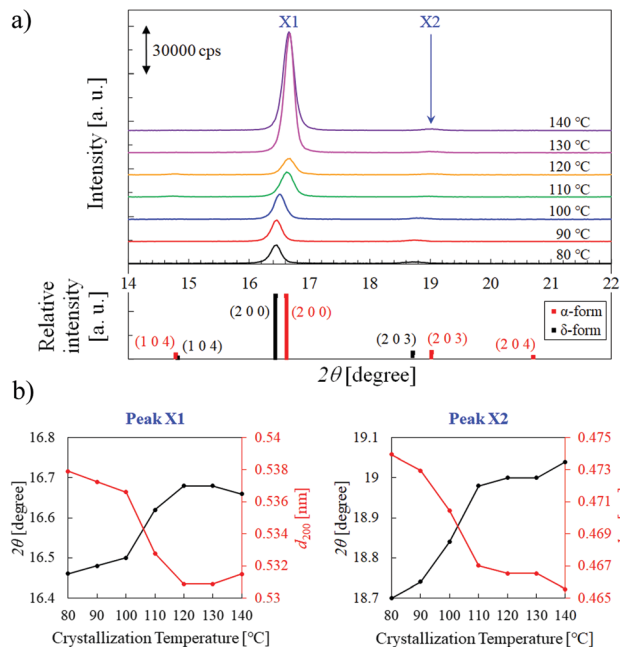


Fig. 4 (a) XRD profiles of PLLA for different crystallization temperature, and standard XRD data of polylactide (JCPDS card no. 64-1623 for δ -form and 64-1624 for α -form). (b) Diffraction angle 2θ of the two peaks labeled in (a). The lattice spacing d_{hkl} values with the Miller indices, calculated by the Bragg equation, are superimposed.

To further optimize the above properties of PLLA, it is important to elucidate the origin of peak B. The remarkable increase of the relative height suggests that probable origin is found not in δ -form but in α -form. According to the literature of PLLA crystalline phases reported by K. Wasanasuk and K. Tashiro's group,¹⁷ the δ -form is not simply the disordered state of the α -form taking the 10_3 helix with 2_1 screw symmetry (the periodic inclusion of 10 monomeric units and the asymmetric inclusion of 5 monomeric units) along the C(CH₃)-C(=O)-O chain axis. Such 2_1 screw symmetry disappears in the δ -form. Therefore, it is natural to consider that the origin of peak B is not due to simply the intermolecular vibration of the PLLA chain but due to a novel intramolecular vibration caused by the 2_1 screw symmetry inside of the helical chain. In contrast, the higher two peaks (C and D), which are existent not only in α -form but also in δ -form, are thought to be the intermolecular vibration of the PLLA chain depending on the lattice spacing and crystallinity. In our future work, the expansion of the observable THz range and detailed structural analysis will deepen our understanding of the PLLA structures and its functions.

Conclusions

Elucidating the optical properties of PLLA is an important issue for predicting its crystal structure and the degree of disorder non-destructively. We prepared, measured, and analyzed PLLA samples with different crystallization temperatures ($T_c = 80$ –140 °C). We introduced the Fourier transform THz spectroscopy to identify differences in the crystal structure among the samples. For the



80 °C samples, four absorption peaks (A, B, C, and D = 1.8, 4.0, 4.7, and 7.1 THz, respectively) were identified in the frequency range of 1.0–8.5 THz, with the peaks of higher T_c samples undergoing blue-shifts. The peak height and width calculations revealed similar temperature dependence for peaks C and D, whereas the peak B height grew remarkably with increasing T_c and could be used as an indicator for PLLA polymorphism optimization. Broadband THz spectroscopy is a powerful tool for various biodegradable polymer materials.

Author contributions

Seiichiro Ariyoshi: conceptualization, methodology, investigation, formal analysis, project administration, writing – original draft. Satoshi Ohnishi: investigation, data curation, formal analysis, writing – review & editing. Hikaru Mikami: investigation, writing – review & editing. Hideto Tsuji: resources, writing – review & editing. Yuki Arakawa: resources, writing – review & editing. Saburo Tanaka: supervision, writing – review & editing. Nobuya Hiroshiba: conceptualization, methodology, investigation, writing – original draft.

Conflicts of interest

There are no conflicts of interest to declare.

Acknowledgements

This work was partly supported by a Grant-in-Aid for Scientific Research (B) [grant number 17H02809] from the Ministry of Education, Culture, Sports, Science and Technology of Japan. The authors would like to thank Mr Kazunobu Yamada from Research and Development Center, Unitika Ltd, for supplying PLLA used in the present study.

References

- 1 B. Žunar, A. Trontel, M. S. Miklenić, J. L. Prah, A. Štafa, N. Marđetko, M. Novak, B. Šantek and I. K. Svetec, *World J. Microbiol. Biotechnol.*, 2020, **36**, 8.
- 2 S. Hama, S. Mizuno, M. Kihara, T. Tanaka, C. Ogino, H. Noda and A. Kondo, *Bioresour. Technol.*, 2015, **187**, 167.
- 3 K. Okano, S. Hama, M. Kihara, H. Noda, T. Tanaka and A. Kondo, *Appl. Microbiol. Biotechnol.*, 2017, **101**, 1869.
- 4 P. Emmanuel Vijay Paul and B. Viswanath, *Recent Developments in Applied Microbiology and Biochemistry*, Academic Press, 2020, ch. 22, 241.
- 5 Y. Tajitsu, *IEEE Trans. Ultrason. Ferroelectr. Freq. Control*, 2008, **55**, 1000.
- 6 E. Fukada, *Rept. Prog. Polym. Phys. Jpn.*, 1991, **34**, 269.
- 7 K. Imoto, M. Date, E. Fukada, K. Tahara, Y. Kamaiyama, T. Yamakita and Y. Tajitsu, *Jpn. J. Appl. Phys.*, 2009, **48**, 09KE06.
- 8 N. Tomoshige, H. Mizuno, T. Mori, K. Kim and N. Matubayasi, *Sci. Rep.*, 2019, **9**, 19514.
- 9 L. Wang, K. Okada, Y. Hikima, M. Ohshima, T. Sekiguchi and H. Yano, *Polymers*, 2019, **11**, 249.
- 10 S. Yamamoto, E. Ohnishi, H. Sato, H. Hoshina, D. Ishikawa and Y. Ozaki, *J. Phys. Chem. B*, 2019, **123**, 5368.
- 11 S. Ariyoshi, B. Setyawan, S. Hashimoto, S. Negishi, H. Mikami and N. Hiroshiba, *RSC Adv.*, 2020, **10**, 8800.
- 12 H. Hoshina, Y. Morisawa, H. Sato, H. Minamide, I. Noda, Y. Ozaki and C. Otani, *Phys. Chem. Chem. Phys.*, 2011, **13**, 9173.
- 13 H. Li, H.-M. Ye and Y. Yang, *Polym. Test.*, 2017, **57**, 52.
- 14 P. Y. Han, M. Tani, M. Usami, S. Kono, R. Kersting and X.-C. Zhang, *J. Appl. Phys.*, 2001, **89**, 2357.
- 15 P. Song, L. Sang, C. Jin and Z. Wei, *Polymer*, 2018, **134**, 163.
- 16 J. Zhang, Y. Duan, H. Sato, H. Tsuji, I. Noda, S. Yan and Y. Ozaki, *Macromolecules*, 2005, **38**, 8012.
- 17 K. Wasanasuk and K. Tashiro, *Polymer*, 2011, **52**, 6097.

